Comparison of Halbach Magnetized Brushless Machines Based on Discrete Magnet Segments or a Single Ring Magnet

Z. Q. Zhu, *Senior Member, IEEE*, Z. P. Xia, *Member, IEEE*, and D. Howe

***Abstract*—This paper compares the air-gap field distribution, cogging torque, back-electromotive-force waveform, and efficiency of brushless machines having a Halbach magnetization produced by either discrete magnet segments or a single ring magnet. Results deduced from finite-element analyses are compared with measurements, and the performance of Halbach magnetized is compared with that of machines equipped with radially magnetized magnets.**

***Index Terms*—Brushless machines, Halbach magnetization, permanent-magnet machines.**

I. Introduction

HALBACH magnetized brushless machines have several attractive features [1]. Most notably, they have an essentially sinusoidal air-gap field distribution and electromotive force (EMF) waveform, and exhibit negligible cogging torque. To date, however, Halbach magnetized machines have generally been fabricated from premagnetized magnet segments having appropriate magnetization orientations [2], which approximates the Halbach magnetization, and, thereby, compromises their performance. However, Halbach magnetized ring magnets, in both sintered and bonded forms, are now available commercially [3], [4]. In this paper, bonded anisotropic Halbach magnetized ring magnets, produced by orientating anisotropic NdFeB powder during the injection moulding process and subsequently impulse magnetizing them with the required Halbach field distribution, are considered, and the performance which results when they are employed in a brushless motor is compared with that which is obtained when the Halbach field is produced by discrete magnet segments and with radially magnetized segments.

II. Halbach Magnetization

In an ideal Halbach magnetized magnet, the magnetization distribution, in polar coordinates ($\vec{e}_r$ and $\vec{e}_\theta$), can be expressed as $\vec{M} = M_r\vec{e}_r + M_\theta\vec{e}_\theta$ where $M_r = M\cos(p\theta)$ and $M_\theta = \pm M\sin(p\theta)$, p being the number of pole-pairs, "$+$" and "$-$" being for internal and external field Halbach cylinders, respectively. However, when a Halbach magnetized magnet is realized from discrete magnet segments, the ideal magnetization distribution is approximated, since the direction of magnetization is fixed in each individual magnet segment by $\theta_m = (1 \pm p)\theta_i$ where θ_i is the angle between $\theta = 0$ and the center of the ith magnet segment (Fig. 1). For example, the magnetization patterns with two and three magnet segments per pole in a 12-pole Halbach magnetized motor are illustrated in Fig. 2.

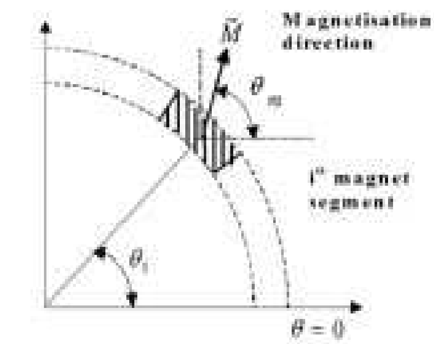

Fig. 1. Angular relationship between θ_m and θ_i.

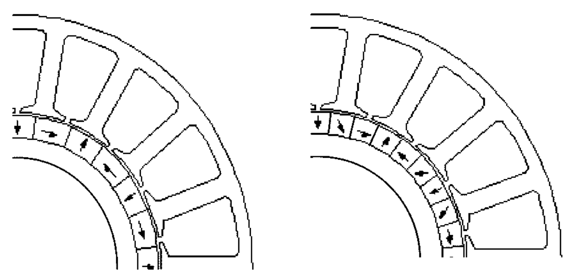

(a) (b)

Fig. 2. Segmented Halbach magnet machine. (a) Two segments/pole. (b) Three segments/pole.

III. Comparison of Alternative Halbach Magnetized Machines

In order to demonstrate the relative merits of brushless machines equipped with ideal and segmented Halbach magnetized rotors, the influence of the number of magnet segments per pole on the field distribution, the cogging torque and the back-EMF waveforms is investigated by finite-element analysis, the torque being obtained by Maxwell stress integration. The motors have identical stators, with an OD = 90 mm, an ID = 55 mm, an axial length = 13 mm, an air-gap length = 0.5 mm, and 18 slots carrying nonoverlapping windings [Figs. 2 and 5(a)]. The segmented Halbach magnet rotors employ sintered NdFeB mag-

Manuscript received February 13, 2002; revised May 21, 2002.

The authors are with the Department of Electronic and Electrical Engineering, University of Sheffield, Sheffield S1 3JD, U.K. (e-mail: Z.Q.Zhu@sheffield.ac.uk; Z.P.Xia@sheffield.ac.uk; D.Howe@sheffield.ac.uk).

Digital Object Identifier 10.1109/TMAG.2002.803190.

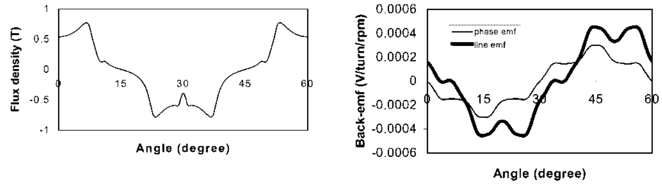

(a)

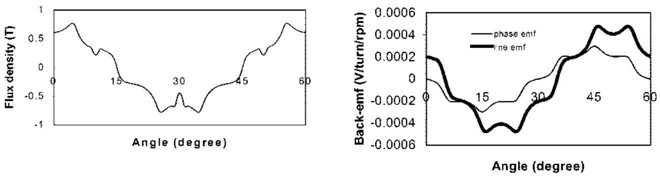

(b)

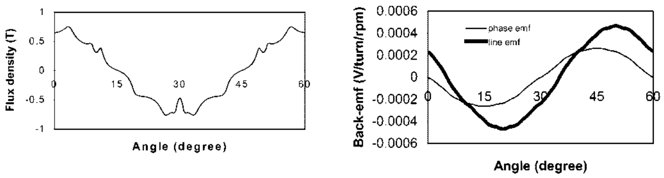

(c)

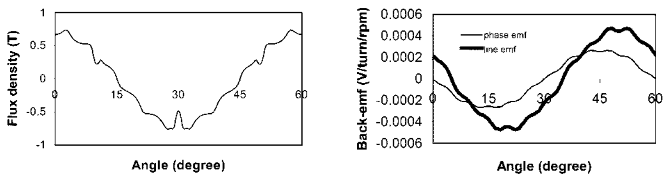

(d)

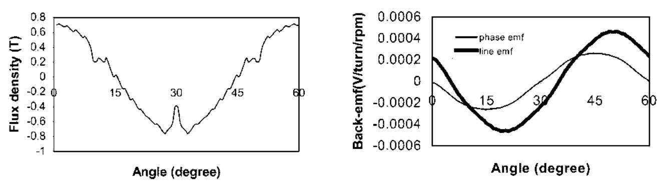

(e)

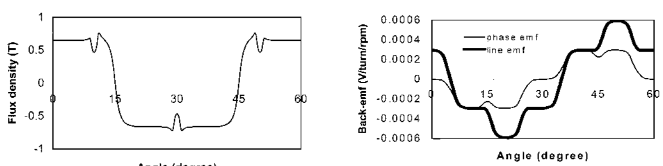

(f)

Fig. 3. Radial air-gap field distributions, and phase and line back-EMF waveforms. (a) Two segments/pole Halbach magnetized. (b) Three segments/pole Halbach magnetized. (c) Four segments/pole Halbach magnetized. (d) Five segments/pole Halbach magnetized. (e) Ideal Halbach magnetized. (f) Radially magnetized (with back-iron).

nets having a remanence of 1.0 T and a radial thickness of 2.4 mm, while the single ring Halbach magnet rotor is an injection-moulded anisotropic NdFeB (NDA502E, 65% loading) magnet [4] having a radial thickness of 4.6 mm, and a remanence of 0.6 T. In this particular paper, the rotors were air-cored. In addition, however, an iron-cored rotor equipped with radially magnetized sintered NdFeB magnets, having a radial thickness of 1.2 mm, was considered. All the motors were designed to meet the same specification, *viz.* 0.71 N·m and 3000 r/min. Al-

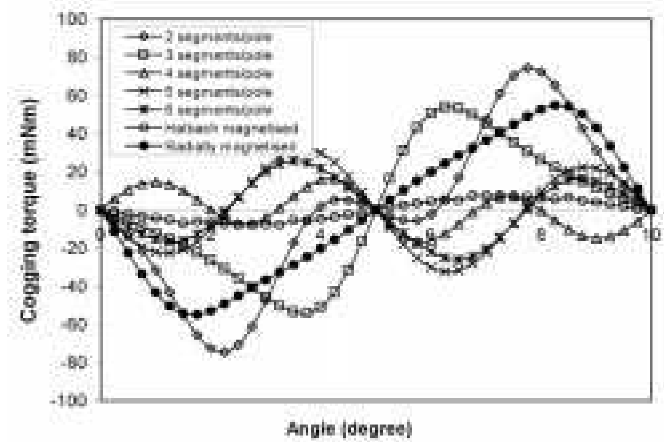

Fig. 4. Cogging torque waveforms.

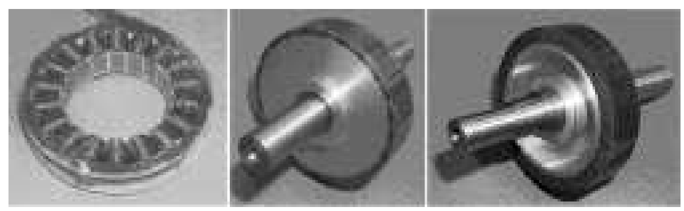

(a) (b) (c)

Fig. 5. Prototype motors. (a) 18-slot, unskewed, nonoverlapping winding stator. (b) 12-pole rotor having two sintered NdFeB magnet segments per pole. (c) 12-pole rotor having a Halbach orientated and magnetized injection-moulded NdFeB ring magnet.

though the materials and the radial thickness of the magnets in three motors are different, they result in a similar saturation level in the stator, while the magnetic loading in the air gap is essentially the same, as shown in Fig. 3.

Finite-element predicted results are shown in Figs. 3 and 4. It can be seen that, in addition to harmonics due to stator slotting, the approximation of the Halbach magnetization introduces significant harmonics in the air-gap field distribution when the number of magnet segments per pole is low. For example, with only two magnet segments per pole, the air-gap field distribution and the back-EMF waveform are much less sinusoidal than that with four or more magnet segments per pole, while the cogging torque is much larger, being similar in magnitude to that which results with radially magnetized magnets. Predictably, as the number of magnet segments per pole is increased, the field distribution and the back-EMF waveform become progressively more sinusoidal, and the cogging torque reduces. With a single ideally magnetized Halbach ring magnet, the motor should exhibit both a sinusoidal air-gap field distribution and a sinusoidal back-EMF waveform, as well as zero cogging torque. However, as will be seen, stator slotting causes a slight distortion, while the resultant cogging torque is not zero (although it is very small) due to inaccuracies in the finite-element calculation, each element being assumed to have a fixed, rather than continuously variable magnetization.

IV. Experimental Results and Discussion

Measurements have been made on two brushless motors having the same stator [Fig. 5(a)] and full-load performance,

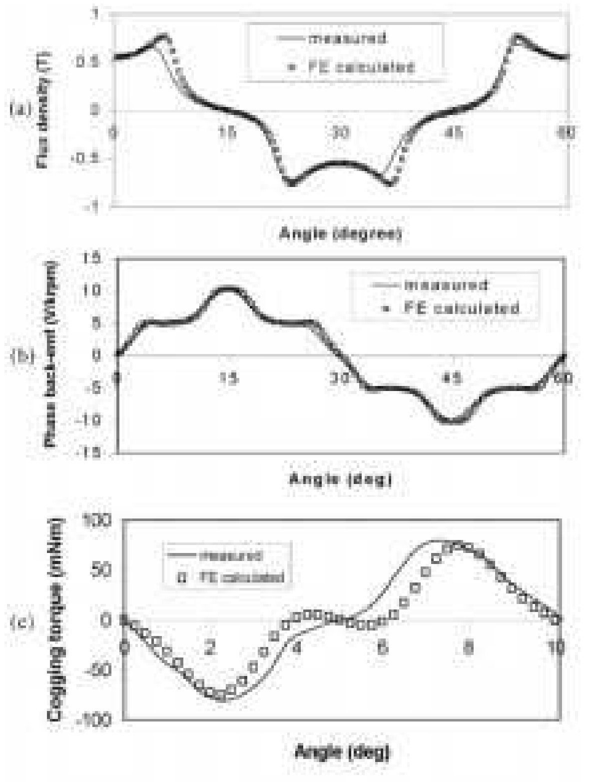

Fig. 6. Comparison of performance of alternative Halbach magnetized motors: two sintered NdFeB magnet segments/pole. (a) Air-gap field distribution. (b) Phase back-EMF waveform. (c) Cogging torque waveform.

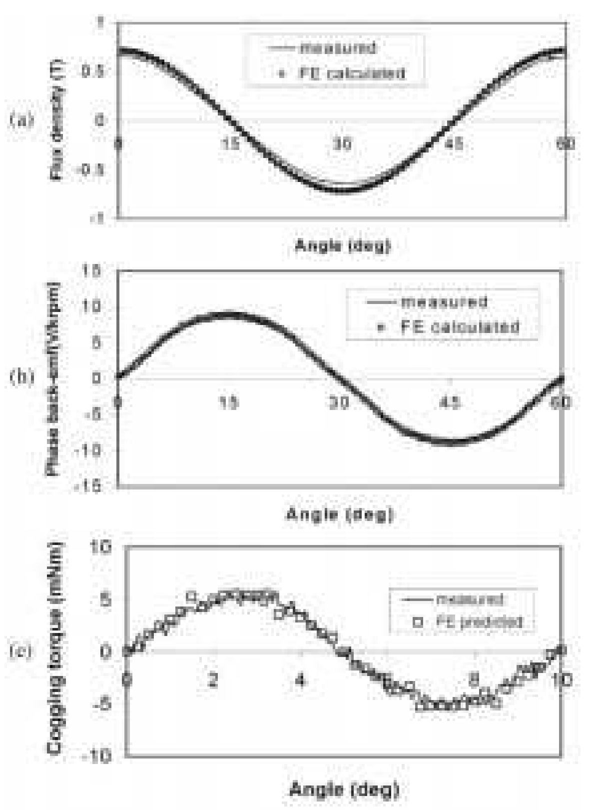

Fig. 7. Comparison of performance of alternative Halbach magnetized motors: anisotropic NdFeB injection-moulded ring magnet. (a) Air-gap field distribution. (b) Phase back-EMF waveform. (c) Cogging torque waveform.

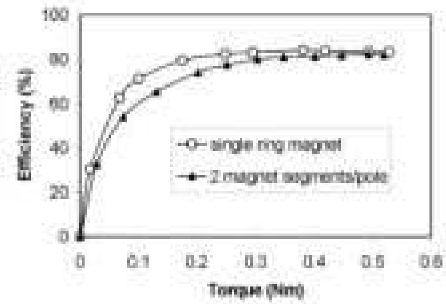

Fig. 8. Measured efficiency–torque characteristics of Halbach magnetized motors.

as specified earlier, but different Halbach magnetized rotors—one having two sintered NdFeB magnet segments per pole [Fig. 5(b)], the other having a Halbach magnetized injection-moulded NdFeB ring magnet [Fig. 5(c)]. Figs. 6–8 compare the measured and predicted air-gap field distributions, the back-EMF, and cogging torque waveforms, and the torque–efficiency characteristics. As will be seen, excellent agreement is achieved for both motors. The main reason for the difference between predicted and measured waveforms for the two magnet segments per pole motor is assembly tolerances. As will be seen, the motor with the Halbach magnetized ring magnet exhibits a very much lower cogging torque (5.5 m·N·m (peak), $<1\%$ of rated torque, in contrast to 80 m·N·m (peak), $\approx 11\%$ of rated torque for the motor with two magnet segments per pole), as well as a higher efficiency, due to its sinusoidal air-gap field distribution, and, therefore, lower stator iron loss.

V. Conclusion

The finite-element method has been used to investigate the performance of Halbach magnetized brushless machines having discrete magnet segments or a single ring magnet. Predicted and measured air-gap field distributions, cogging torque and back-EMF waveforms, and efficiency, have been compared, and excellent agreement has been achieved. It has been shown that since segmented Halbach magnets approximate the Halbach magnetization, they compromise the performance of the motors in which they are employed, although the use of a higher number of magnet segments per pole improves the field distribution, albeit increasing the cost of fabrication.

References

[1] K. Halbach, “Design of permanent magnet multipole magnets with oriented rare earth cobalt material,” *Nucl. Instrum. Methods*, vol. 169, pp. 1–10, 1980.

[2] M. Marinescu and N. Marinescu, “New concept of permanent magnet excitation for electrical machines—Analytical and numerical computation,” *IEEE Trans. Magn.*, vol. 28, pp. 1390–1393, Mar. 1992.

[3] K. Atallah and D. Howe, “The application of Halbach cylinders to brushless ac servo motors,” *IEEE Trans. Magn.*, vol. 34, pp. 2060–2062, July 1998.

[4] Z. Q. Zhu, Z. P. Xia, K. Atallah, G. W. Jewell, and D. Howe, “Powder alignment system for anisotropic bonded NdFeB Halbach cylinders,” *IEEE Trans. Magn.*, vol. 36, pp. 3349–3352, Sept. 2000.